This decrease reflects the fact that the angle ϕ corresponding to the conformational minimum of pipecolic acid, while also negative, has a much greater absolute magnitude than that observed for Ala at this position (*21*). The significantly lower stability of the mutant enzyme containing the isoelectronic hydroxy analog of Ala, **3**, is surprising because the NH of Ala is hydrogen-bonded to water and not to another residue in the protein. In addition, although ester bonds have lower barriers to cis-trans isomerization than amides, they are strongly biased toward the planar trans conformation (*22*). The lower melting temperature may reflect the fact that the ester carbonyl is a much weaker hydrogen-bond acceptor than the analogous amide carbonyl (*23*).

The stabilities of most of the mutant enzymes were also evaluated by correlation of heat and time of inactivation (Fig. 3) (*4, 24*). Although less accurate than the CD determination, this method was more convenient because the assay could be carried out directly with the unpurified in vitro reaction supernatant. Control experiments demonstrated that protein obtained by in vitro suppression of the amber 82 mutation with Pro was approximately 1° to 2°C more stable than wild-type protein, in agreement with previous reports (*4, 25*). Qualitatively, the results agreed with the relative stabilities obtained by the CD experiments, with lactic acid as the least stable mutant. The two mutant enzymes containing **9** and **11** were both close in stability to the wild-type enzyme. It appears from these and the CD melting study results that the electronic properties of substitutions at position 82 of T4L have a greater effect on protein stability than the conformational restrictions caused by substitutions.

We have demonstrated that proteins containing significant modifications to the polypeptide backbone can be synthesized and purified and that their thermal properties can be characterized. These results suggest that it should be possible to systematically survey the effect of a wide range of amino acids containing backbone and side-chain perturbations in order to more precisely evaluate the factors that are important for protein stability.

REFERENCES AND NOTES

1. C. J. Noren, S. J. Anthony-Cahill, M. C. Griffith, P. G. Schultz, *Science* **244**, 182 (1989).
2. J. Ellman, D. Mendel, C. J. Noren, S. Anthony-Cahill, P. G. Schultz, *Methods Enzymol.*, in press.
3. T. Alber and B. W. Matthews, *ibid.* **154**, 511 (1987); X. -J. Zhang *et al.*, *Biochemistry* **30**, 2012 (1991), and references therein.
4. B. W. Matthews, H. Nicholson, W. J. Becktel, *Proc. Natl. Acad. Sci. U.S.A.* **84**, 6663 (1987).
5. C. J. Noren *et al.*, *Nucleic Acids Res.* **18**, 83 (1990).
6. D. Mendel, J. A. Ellman, P. G. Schultz, *J. Am. Chem. Soc.* **113**, 2758 (1991).
7. Plasmid pHSe54,97.TA encodes a cysteine-free T4L behind a twin *tac* promoter and was kindly provided by L. McIntosh of the Dahlquist group at the University of Oregon. The cysteine-free version of T4L is virtually identical to the wild-type in structure and activity but does not suffer oxidative degradation [L. J. Perry and R. Wetzel, *Biochemistry* **25**, 733 (1986); *Protein Eng.* **1**, 101 (1987)].
8. J. R. Sayers, W. Schmidt, F. Eckstein, *Nucleic Acids Res.* **16**, 791 (1988).
9. Two isoforms of the enzyme produced in vitro are observed in the expression driven by pHSe54,97.TA, one of which is identical to the protein obtained by suppression of pT4L82am with Ala.
10. Supernatants (2 μl) from suppression reactions were mixed with 1.0 ml of an ~500 μg ml^{-1} suspension of *E. coli* strain NAPIV cells [M. A. Nelson and L. Gold, *Mol. Gen. Genet.* **188**, 69 (1982)] in 50 mM tris · HCl, 1 mM EDTA, pH 7.4, and the change in absorbance at 450 nm was plotted as a function of time.
11. S. A. Robertson, J. A. Ellman, P. G. Schultz, *J. Am. Chem. Soc.* **113**, 2722 (1991).
12. We have attempted to suppress D-alanine as well as other D–amino acids at several sites in a number of proteins and have yet to detect any incorporation.
13. A. Bhuta *et al.*, *Biochemistry* **20**, 8 (1981).
14. P. Bhuta *et al.*, *ibid.* **21**, 899 (1982).
15. T. Yamane *et al.*, *ibid.* **20**, 7059 (1981).
16. S. Fahnestock, H. Weissbach, A. Rich, *Biochim. Biophys. Acta* **269**, 62 (1972).
17. J. D. Bain *et al.*, *Biochemistry* **30**, 5411 (1991); S. Fahnestock and A. Rich, *Science* **173**, 340 (1971).
18. W. J. Becktel and W. A. Baase, *Biopolymers* **26**, 619 (1987).
19. The buffer used for the CD measurements was that described by P. Connelly *et al.* [*Biochemistry* **30**, 1887 (1991)].
20. Y. Paterson *et al.*, *J. Am. Chem. Soc.* **103**, 2947 (1981); E. Benedetti *et al.*, *Biopolymers* **28**, 175 (1989).
21. Within peptides, the carboxyl group of pipecolic acid occupies the axial position in the cyclohexane chair conformation to avoid the unfavorable axial 1,3 steric interactions between the carboxyl group and the acylamide linkage when the carboxyl group is in the equatorial position [M. K. Rosen, R. F. Standaert, A. Galat, M. Nakatsuka, S. L. Schreiber, *Science* **248**, 863 (1990); I. D. Rae and H. A. Scheraga, *Int. J. Pept. Protein Res.* **13**, 304 (1979)].
22. K. B. Wiberg and K. E. Laidig, *J. Am. Chem. Soc.* **109**, 5935 (1987).
23. M. J. Kamlet, J.-L. M. Abboud, M. H. Abraham, R. W. Taft, *J. Org. Chem.* **48**, 2877 (1983); M. D. Joesten and L. J. Schaad, *Hydrogen Bonding* (Dekker, New York, 1974), pp. 309–335.
24. J. A. Wells and D. B. Powers, *J. Biol. Chem.* **261**, 6564 (1986).
25. The pH for the temperature versus time of inactivation experiments was 6.5, whereas the pH for the CD experiments was 2.51.

26. We are grateful to Z. Chang for help in the synthesis of several of the amino acyl pdCpA derivatives. Supported by Office of Naval Research grant N00014-87-K-0256 (J.A.E.), and by the Director, Office of Energy Research, Office of Basic Energy Sciences, Division of Material Sciences and the Division of Energy Biosciences of the U.S. Department of Energy (DE-AC03-76SF00098) (D.M.). D.M. was supported by American Cancer Society postdoctoral fellowship PF-4014 and J.A.E. by NSF postdoctoral fellowship CHE-8907488. P.G.S. is a W. M. Keck Foundation Investigator.

28 August 1991; accepted 21 October 1991

Optical Analysis of Synaptic Vesicle Recycling at the Frog Neuromuscular Junction

WILLIAM J. BETZ* AND GUY S. BEWICK†

The fluorescent dyes FM1-43 and RH414 label motor nerve terminals in an activity-dependent fashion that involves dye uptake by synaptic vesicles that are recycling. This allows optical monitoring of vesicle recycling in living nerve terminals to determine how recycled vesicles reenter the vesicle pool. The results suggest that recycled vesicles mix with the pool morphologically and functionally. One complete cycle of release of transmitter, recycling of a vesicle, and rerelease of transmitter appears to take about 1 minute.

SECRETION OF ACETYLCHOLINE (ACh) from motor nerve terminals occurs through exocytosis of synaptic vesicles at specific sites (active zones), after which vesicle membranes are recaptured, refilled with transmitter, and returned to the pool of vesicles clustered near the active zone. This process, known as vesicle recycling (*1*), is common to all chemically transmitting synapses but is not well understood. We wanted to determine whether recycled vesicles freely mix with the vesicle pool or are preferentially routed to a specific region of the pool (Fig. 1A). To study vesicle recycling, we used styryl dyes to label nerve terminals in an activity-dependent fashion; the dyes mark recycled vesicles (*2, 3*). Transmitter release during or just preceding exposure to the dye must occur for the terminal to be labeled.

The fluorescent labeling pattern in living frog cutaneus pectoris preparations consists of a series of discrete spots 1 to 2 μm in diameter, distributed like beads along the length of motor nerve terminals (*2*). The spots align with postsynaptic ACh receptors and disappear if the nerve is stimulated in dye-free medium. The size and number of spots match the immunocytochemical distribution of synapsin I (*4*) and ultrastructural observations of synaptic vesicle clusters.

Department of Physiology, University of Colorado School of Medicine, Denver, CO 80262.

*To whom correspondence should be addressed.
†Present address: Muscular Dystrophy Research Laboratories, Newcastle General Hospital, Newcastle-Upon-Tyne, NE4 6BE, United Kingdom.

These and other observations (*2*) suggest that the fluorescent spots consist of clusters of stained recycled vesicles. We assumed that the brightness of the spots was proportional to the number of labeled vesicles and that destaining was a result of dye loss by exocytosis of labeled vesicles.

To determine how recycling vesicles reenter the vesicle pool, we compared the staining pattern obtained with partial dye loading to that obtained with full dye loading (Fig. 1B). Terminals were loaded by exposure to the dye, and partial loading was produced by shortening the exposure time (*5*). If recycled vesicles mix with the entire vesicle pool, the fluorescent spots in partially loaded terminals should be as large in diameter as those in fully loaded terminals but less fluorescent. If, on the other hand, recycled vesicles are sequestered in one part of the pool, the partially loaded spots should be as fluorescent as those in fully loaded terminals but smaller in diameter. To obtain information in three dimensions, we studied some terminals that lay on the top surface of the muscle fiber they innervated and others that lay on the side. The spots in partially loaded terminals were about the same size as, but less bright than, those in fully loaded terminals, suggesting that the recycled vesicles distributed throughout the vesicle pool. The experiment was also performed with two dyes that could be imaged independently and similar results were obtained (Fig. 1C).

Although there appeared to be no spatial sequestration of recycled vesicles, recycled vesicles still might differ functionally from other vesicles. To determine if the morphological mixing (Fig. 1) reflected functional mixing, we destained fully loaded terminals in two stages (terminals destained only during nerve stimulation) (Fig. 2). The nerve was stimulated, and after about one-half of the dye had disappeared, stimulation was halted for 10 min and then resumed. The initial rates of destaining during the two stimulation periods were then compared. If vesicles recycled functionally to the back of the pool, the destaining rate during the second period should be the same as during the first; if recycled vesicles were preferentially rereleased, there should be a lag in destaining at the beginning of the second stimulation period. If recycled vesicles mixed functionally with the pool, the rate of destaining should be slowed by a predictable amount as the pool becomes diluted with unlabeled vesicles.

The rate of dye loss was slower during the second stimulation period than during the

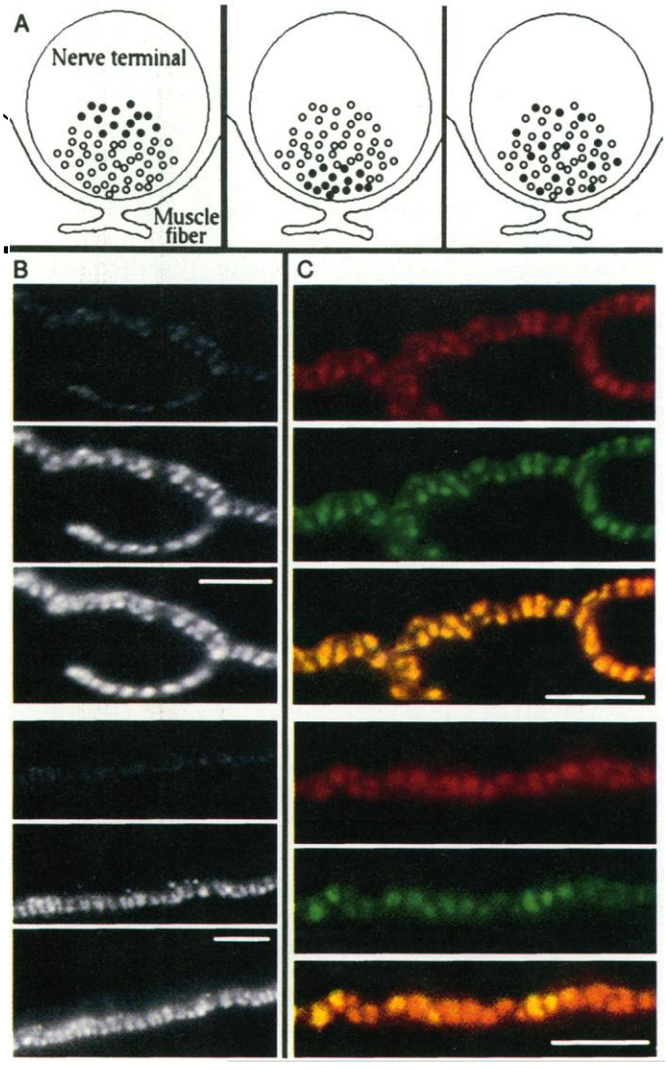

Fig. 1. Morphological mixing of recycled vesicles within the vesicle pool. (**A**) Illustration of how stained, recycled vesicles (filled circles) might reenter the vesicle pool (open circles). (Left) Reentry at the back of the pool. (Middle) Reentry at the front of the pool. (Right) Mixing within the pool. (**B**) Images of terminals acquired after partial and full dye loading. One terminal lay on the top surface of the muscle fiber it innervated (top three panels) and one lay on the side (bottom three panels). The brightness of the top (partial load) and bottom (full load) images in each set of three panels is directly comparable (partially loaded terminals were about one-fourth as bright as fully loaded terminals). The middle image is the partially loaded image digitally enhanced to about the same brightness as the fully loaded image. (**C**) Two terminals [top and side views as in (B)] labeled with RH414 (red) and FM1-43 (green). These two terminals were first fully loaded with RH414 and imaged. They were then partially loaded with FM1-43 and reimaged with optics that excluded any signal from RH414. The two images were processed independently for optimum contrast and then superimposed (lowest panel of each set of three). Regions of overlap of the red and green images appear yellow. It is clear that the spots, whether lightly or heavily stained, overlap with considerable precision. All scale bars = 5 μm.

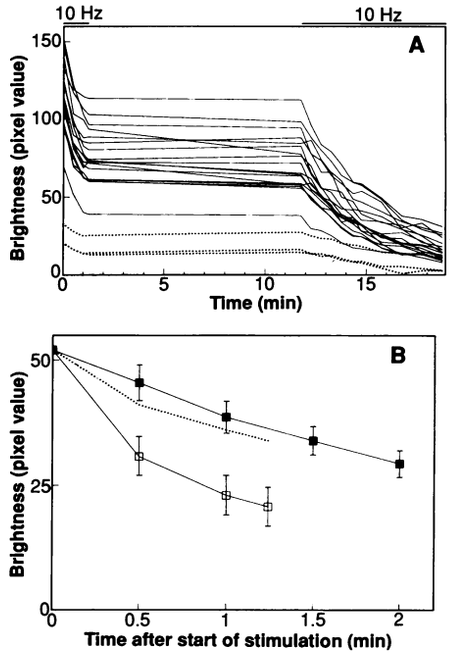

Fig. 2. Functional mixing of recycled vesicles within the vesicle pool. (**A**) Terminals were loaded with dye and repeatedly imaged. The nerve was stimulated at 10 Hz during the times indicated. Images were processed identically and aligned. The brightness of 15 fluorescently labeled spots (solid lines) and three background areas (dotted lines) is plotted against time. (**B**) To facilitate comparison of the initial rates of destaining during the two stimulation periods, results in (A) were background-subtracted, averaged, and plotted so that the first point of each stimulation period coincided. Open squares (mean ± SEM) show first stimulation period. Dotted line shows predicted brightness during second stimulation period, assuming that vesicles released during the first stimulation period lost their dye, recycled, and mixed randomly with the remaining labeled vesicles during the 10-min rest period. Filled squares (mean ± SEM) show observed brightness during second stimulation period.

first. If we assume that the terminal returned to its original functional state during the rest period (so that the excitability state and number of vesicles returned to initial conditions) and that recycled vesicles mixed randomly with the vesicle pool, the amount of slowing can be predicted. At the start of the second stimulation period, the average brightness had decreased by 42%. Thus, if random mixing occurred, the initial rate of dye loss during the second stimulation period should be 42% lower than during the first stimulation period (Fig. 2B, dotted line). The observed rate (Fig. 2B, filled squares) was only slightly slower than this and is thus consistent with the hypothesis that recycled vesicles mixed randomly both morphologically and functionally with vesicles in the pool.

If terminals did not recover fully during the rest period and less transmitter was released during the second stimulation period (*6*), then the slower rate of dye loss could reflect reduced transmitter release. To test this possibility, we performed two-stage destaining of fully loaded terminals with simultaneous monitoring of end plate potentials (EPPs) (Fig. 3A) and fluorescent spots (Fig. 3B). EPP peak amplitudes were summed as a measure of cumulative transmitter release, and we scaled them to match the dye-loss plateau during the rest period (Fig. 3C, dotted line). The total amount of destaining during the first stimulation period was about 32%. If we assume random recycling of vesicles, the rate of dye loss during the second period should be about 32% less than the rate of transmitter release. The solid line (Fig. 3C) is drawn according to this prediction and fits the observed destaining rate well. Figure 3 also shows that EPPs summed less rapidly during the second stimulation period than during the first (*6*), indicating that transmitter release was slightly reduced. This could explain why in Fig. 2B the observed destaining rate was slightly lower than predicted.

We next measured the time required for one complete cycle of transmitter release, vesicle recycling, and rerelease of transmitter by comparing dye loss and transmitter release during a single period of uninterrupted stimulation (Fig. 4). Terminals fully loaded with dye were stimulated, and the rates of transmitter release (summed EPPs) and dye loss were measured as in Fig. 3. After about 1 min, the rate of dye loss fell below that of transmitter release, which may reflect synaptic vesicle recycling. That is, if vesicles lost their dye during exocytosis and randomly reentered the vesicle pool, then the rate of dye loss would begin to lag behind the rate of transmitter release as second-generation vesicles (unlabeled) began to discharge along with older (labeled) vesicles. The solid line (Fig. 4) is drawn according to such a model (7) and fits the observed rate of dye loss.

We have described our results in terms of the vesicular hypothesis of transmitter release although these experiments give no evidence of individual stained vesicles or quantization of dye release. Thus, one might alternatively suppose that the dye is free in the cytoplasm and escapes from the terminals through an activity-dependent membrane transporter (*8*). However, for this idea to be valid, the observed staining pattern (discrete fluorescent spots) would require that dye distribution in the cytoplasm be tightly constrained to regions of synaptic vesicle clusters, which seems unlikely. Moreover, our results agree well with ultrastructural studies of vesicle recycling. For example, after frog cutaneus pectoris nerve terminals were stimulated at 10 Hz for 1 min, total vesicle numbers were reduced by about 35%, and about 10% of the vesicles had recycled (*9*). Similarly, we found that stimulation at 10 to 20 Hz for 1 min caused the loss of 30 to 40% of the dye and produced only the initial signs of recycled vesicles.

Ultrastructural studies of uptake of horseradish peroxidase by frog motor nerve terminals show labeled vesicles mixed with the population of unlabeled vesicles without signs of sequestration (*6, 9, 10*). Our results are consistent with this morphological observation and extend it to a functional level. On the other hand, biochemical studies of transmitter release show evidence of preferential release of newly synthesized transmitter (*11, 12*), which has been interpreted as reflecting the existence of multiple transmitter-containing compartments with different turnover rates. Further biochemical evidence has shown that synaptic vesicles are not uniform but comprise at least two distinct populations (*13*). It has been suggested that one vesicle population is preferentially released and recycled, whereas another forms a reserve pool that turns over more slowly (*14*). We saw no evidence of a reserve

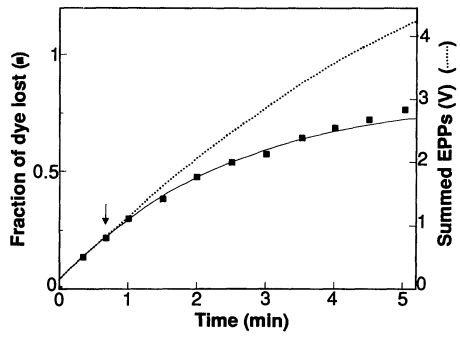

Fig. 4. Recycle time is about 1 min. EPPs and images were recorded during continuous uninterrupted nerve stimulation and plotted as in Fig. 3C. The dotted line shows summed EPP amplitudes (corrected for nonlinear summation). Squares show average dye loss from four spots (after background was subtracted). The ordinates were scaled so that the two curves superimposed at the early times. The solid line is drawn according to a model (7) that assumes that a vesicle requires a fixed amount of time after release (40 s; arrow) before recycling randomly into the vesicle pool.

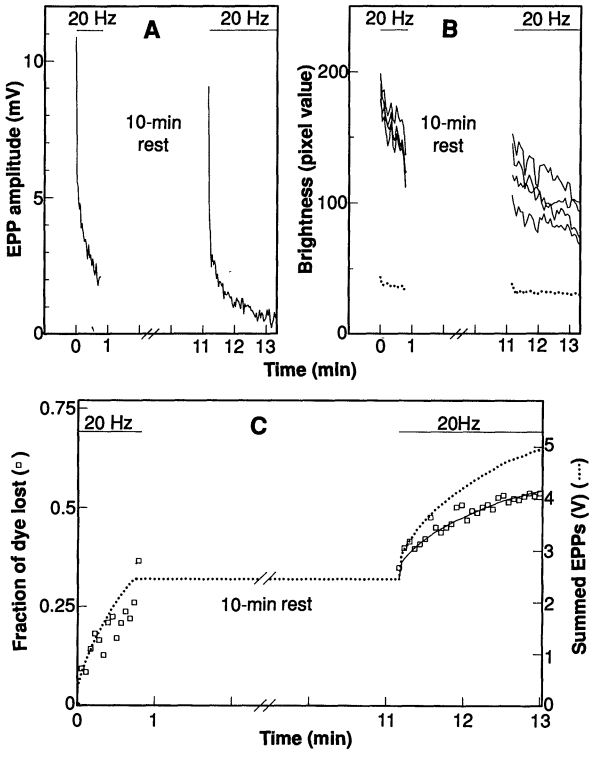

Fig. 3. Simultaneous measurement of fluorescence and EPPs. Nerve stimulation (20 Hz) was applied for about 50 s, halted for 10 min, and resumed. (**A**) EPP amplitudes during the two stimulation periods. (**B**) Brightness of four fluorescent spots (solid lines) and background area (dotted line) during destaining. (**C**) Squares show average fraction of dye lost from spots. The dotted line shows the summed amplitude of EPPs (corrected for nonlinear summation; corrections were less than 10%) scaled to match the average dye loss (32%) after the end of the first stimulation period. The solid line is drawn according to $y' = 0.68\,(y - 0.32) + 0.32$ where y = observed summed EPP amplitude (dotted line), and y' = predicted dye loss, assuming that 32% of vesicles were released during the first stimulation period, were recycled without dye, and were mixed randomly with the remaining dye-filled vesicles.

pool; although our results do not rule out the existence of a small reserve pool, our results can be quantitatively described by a simple model involving spatially random recycling into a uniform pool of vesicles.

How could vesicle mixing occur? Vesicles are clearly constrained at rest in discrete clusters, and evidence suggests that, within each cluster, individual vesicles are bound to a filamentous meshwork consisting, at least in part, of the protein synapsin I (*4, 15*). It has been suggested that during activity vesicles detach from synapsin I (*16*), but the observation that fluorescent dye spots do not blur during destaining (*2*) suggests that vesicles are still constrained in some way during activity. If they are actively moved to the presynaptic membrane (for example, by a molecular motor linked to the cytoskeleton), the present results suggest that recycling vesicles must be able to enter this queue at any location. This could happen if, for example, mature vesicles reappeared [for example, by budding from cisternae and by the removal of clathrin coats (*1*)] at random locations within the cluster.

REFERENCES AND NOTES

1. J. E. Heuser, *Q. J. Exp. Physiol.* **74**, 1051 (1989); F. Valtorta *et al.*, *Neuroscience* **35**, 477 (1990); F. Torri Tarelli, F. Valtorta, A. Villa, J. Meldolesi, *Prog. Brain Res.* **84**, 83 (1990).
2. W. J. Betz and G. S. Bewick, *Soc. Neurosci. Abstr.* **16**, 53 (1990); W. J. Betz, F. Mao, G. S. Bewick, *J. Neurosci.* **12**, 363 (1992).
3. W. J. Betz and G. S. Bewick, *Soc. Neurosci. Abstr.* **17**, 1157 (1991).
4. F. Valtorta *et al.*, *Neuroscience* **24**, 593 (1988).
5. Experiments were performed on acutely dissected frog cutaneus pectoris nerve muscle preparations as described (*2*). Briefly, muscles were stained by exposure to FM1-43 (1 to 2 μM) or RH414 (40 μM) in bathing solution containing 60 mM KCl, 55 mM NaCl, 1.8 mM $CaCl_2$, and 2.4 mM $NaHCO_3$ and then washed in normal Ringer's solution (2 mM KCl, 115 mM NaCl, 1.8 mM $CaCl_2$, and 2.4 mM $NaHCO_3$). For the experiments in Fig. 1, $[K^+]$ was 25 mM during staining, and terminals were exposed to dye for 2 min (partial load) or 5 min (full load). We used curare (3 to 9 μM) to block muscle contractions. Images were obtained with a Leitz Laborlux epifluorescence microscope with a 100-W Hg lamp and 1 to 10% neutral density transmission filters. Carl Zeiss ×40 water immersion and ×63 oil immersion objectives (0.75 and 1.4 numerical aperture, respectively) were used. Optics for FM1-43 included a 430- to 440-nm band-pass excitation filter, a Leitz H3 dichroic mirror, and a 500- to 600-nm band-pass emission filter. Optics for RH414 included a 541- to 551-nm band-pass excitation filter, a Leitz N2 dichroic mirror, and a 600- to 700-nm band-pass emission filter. Optics for FM1-43 in Fig. 1C included a 450- to 550-nm band-pass emission filter. Control observations of terminals stained with only one dye showed that spectral separation of the two dyes was virtually complete under these conditions. Under optimal conditions, RH414 is invisible in the 450- to 550-nm range, but FM1-43 can be detected in the 500- to 600-nm range. Thus, terminals were stained and imaged first with RH414. Only terminals on surface muscle fibers were studied. Images were captured with a Star I camera (3-s exposure; gain 4) (Photometrics Ltd., Tucson, AZ) and were stored and processed with a Personal Iris computer (Silicon Graphics, Mountain View, CA) running software from G. W. Hannaway and Associates (Boulder, CO). Images in any single destaining experiment were processed identically and aligned. We marked spots to be measured on the first image, and average spot intensities were then computed for each image. We used conventional intracellular recording methods to measure EPPs. Overillumination slows dye release, but the safety factor is large enough to ensure that many consecutive images can be obtained without signs of phototoxicity (*2*). In these experiments, illumination times and intensities were well below levels at which such effects are observed.
6. B. Ceccarelli, W. P. Hurlbut, A. Mauro, *J. Cell Biol.* **57**, 499 (1973).
7. The solid line in Fig. 4 was calculated through an iterative process based on the following assumptions. (i) Vesicles were uniformly labeled with dye at time zero. (ii) Labeled vesicles lost all dye during exocytosis. (iii) After exocytosis, vesicles were recycled after a time t_r of 40 s. (iv) Recycled vesicles mixed randomly within the vesicle pool. (v) Labeled and unlabeled vesicles released the same amount of transmitter. (vi) The slope of the scaled, summed EPP curve (Fig. 4, dotted line) reflected the amount of transmitter released at any given time. All calculations were made as fractions of the initial dye brightness (after background was subtracted). At t = 40 s, 21% of the dye signal had been lost. Thus 79% of the initial number of vesicles remained (all labeled), and unlabeled vesicles began to reenter the pool at a rate given by the slope of the summed EPP curve at time zero. Iterations were calculated every 2 s. At each time point t, the fraction of vesicles reentering the pool was calculated from the slope of the EPP curve at $t - t_r$, the fractions of labeled and unlabeled vesicles in the pool were recalculated, and the predicted fraction of dye lost (Fig. 4, solid line) was computed from the slope of the EPP curve at time t.
8. M. Israel, N. Morel, B. Lesbats, S. Birman, R. Manaranche, *Proc. Natl. Acad. Sci. U.S.A.* **83**, 9226 (1986); M. Israel, B. Lesbats, M. Sbia, N. Morel, *J. Neurochem.* **55**, 1758 (1990).
9. J. E. Heuser and T. S. Reese, *J. Cell Biol.* **57**, 315 (1973).
10. B. Ceccarelli *et al.*, *ibid.* **54**, 30 (1972).
11. I. J. Kopin *et al.*, *J. Pharmacol. Exp. Ther.* **161**, 271 (1968); B. Collier and F. C. MacIntosh, *Can. J. Physiol. Pharmacol.* **47**, 127 (1969); L. T. Potter, *J. Physiol. (London)* **206**, 145 (1970).
12. H. Zimmermann, *Neuroscience* **4**, 1773 (1979).
13. V. P. Whittaker, *Prog. Brain Res.* **84**, 419 (1990); H. Zimmermann, *Handb. Exp. Pharmacol.* **86**, 349 (1988).
14. L. A. Barker, *Biochem. J.* **130**, 1063 (1972); V. P. Whittaker, *Ann. N.Y. Acad. Sci.* **493**, 77 (1987); H. Zimmerman *et al.*, *Cell Biol. Int. Rep.* **13**, 993 (1989).
15. F. Navone, P. Greengard, P. DeCamilli, *Science* **226**, 1209 (1984); W. Schiebler *et al.*, *J. Biol. Chem.* **261**, 8383 (1986); D. M. D. Landis *et al.*, *Neuron* **1**, 201 (1988); N. Hirokawa, K. Sobue, K. Kanda, A. Harada, H. Yorifuji, *J. Cell Biol.* **108**, 111 (1989).
16. R. Llinas, T. L. McGuinness, C. S. Leonard, M. Sugimori, P. Greengard, *Proc. Natl. Acad. Sci. U.S.A.* **82**, 3035 (1985); R. Llinas *et al.*, *J. Physiol. (London)* **436**, 257 (1991).

17. We thank S. Fadul for technical assistance and B. Wallace, P. Fuchs, and H. Gates for helpful comments on the manuscript. Supported by NIH grants NS10207 and NS23466 (to W.J.B.).

20 September 1991; accepted 11 November 1991

Dimerization of a Specific DNA-Binding Protein on the DNA

BAEK KIM AND JOHN W. LITTLE

Many specific DNA-binding proteins bind to sites with dyad symmetry, and the bound form of the protein is a dimer. For some proteins, dimers form in solution and bind to DNA. LexA repressor of *Escherichia coli* has been used to test an alternative binding model in which two monomers bind sequentially. This model predicts that a repressor monomer should bind with high specificity to an isolated operator half-site. Monomer binding to a half-site was observed. A second monomer bound to an intact operator far more tightly than the first monomer; this cooperativity arose from protein-protein contacts.

THE BINDING SITES FOR MANY SPECIFIC DNA-binding proteins have dyad symmetry (*1, 2*), and x-ray crystallographic studies of several DNA-protein complexes show that one subunit of a dimer contacts each half of the operator (*2, 3*). For many proteins, these complexes form by binding of preformed dimers to their sites. It is not certain, however, that this is true in all cases. Indeed, several such proteins do not detectably dimerize in solution (*2*), or they dimerize weakly as in the case of LexA, a bacterial transcriptional repressor (*4, 5*).

LexA, which represses the SOS regulon (*6*), is similar to the cI repressor of bacteriophage λ, both in the sequence of its COOH-terminal domain and in its general organization. Its NH_2-terminal domain binds DNA (*7, 8*); the COOH-terminal domain provides most of the contacts for dimerization, because the in vitro dissociation constant for dimer formation in solution (K_{dimer}) is about the same for both the COOH-terminal domain and intact LexA (*4, 5*). However, the value of K_{dimer}, ≈50 μM, is so high that the concentration of dimers in in vitro experiments is low. This suggests that the pathway for binding of dimers to DNA (Fig. 1A, pathway I) cannot account for the rapid rate at which LexA

B. Kim, Department of Biochemistry, University of Arizona, Tucson, AZ 85721.
J. W. Little, Departments of Biochemistry and Molecular and Cellular Biology, University of Arizona, Tucson, AZ 85721.